NAVAL POSTGRADUATE SCHOOL

MONTEREY, CALIFORNIA

THESIS

TUNING, VALIDATION, AND UNCERTAINTY ESTIMATES FOR A SOUND EXPOSURE MODEL

by

Francis J. Carmody

September 2011

Thesis Co-Advisors: John Joseph
Ching-Sang Chiu

Approved for public release; distribution is unlimited

THIS PAGE INTENTIONALLY LEFT BLANK

REPORT DOCUMENTATION PAGE			*Form Approved OMB No. 0704-0188*
Public reporting burden for this collection of information is estimated to average 1 hour per response, including the time for reviewing instruction, searching existing data sources, gathering and maintaining the data needed, and completing and reviewing the collection of information. Send comments regarding this burden estimate or any other aspect of this collection of information, including suggestions for reducing this burden, to Washington headquarters Services, Directorate for Information Operations and Reports, 1215 Jefferson Davis Highway, Suite 1204, Arlington, VA 22202-4302, and to the Office of Management and Budget, Paperwork Reduction Project (0704-0188) Washington DC 20503.			
1. AGENCY USE ONLY ***(Leave blank)***	**2. REPORT DATE** September 2011	**3. REPORT TYPE AND DATES COVERED** Master's Thesis	
4. TITLE AND SUBTITLE Tuning, Validation, and Uncertainty Estimates for a Sound Exposure Model		**5. FUNDING NUMBERS**	
6. AUTHOR(S) Francis J. Carmody			
7. PERFORMING ORGANIZATION NAME(S) AND ADDRESS(ES) Naval Postgraduate School Monterey, CA 93943-5000		**8. PERFORMING ORGANIZATION REPORT NUMBER**	
9. SPONSORING /MONITORING AGENCY NAME(S) AND ADDRESS(ES) N/A		**10. SPONSORING/MONITORING AGENCY REPORT NUMBER**	
11. SUPPLEMENTARY NOTES The views expressed in this thesis are those of the author and do not reflect the official policy or position of the Department of Defense or the U.S. Government. IRB Protocol number _____N/A_____.			
12a. DISTRIBUTION / AVAILABILITY STATEMENT Approved for public release; distribution is unlimited		**12b. DISTRIBUTION CODE**	

13. ABSTRACT (maximum 200 words)

To tune and validate the performance of an acoustic model, sound signals were transmitted from a calibrated source, at varied mid-range frequencies, and received on a moored acoustic recording package at the edge of Tanner Bank near the Southern California Anti-Submarine Warfare Range (SOAR). The acoustic monitoring package was constructed of three calibrated Acousonde recorders. Source levels (SL) were measured at 1.8 meters from the source using a Bioacoustic Probe. Signals recorded on the Acousondes and the Bioacoustic Probe were processed to measure transmission loss (TL) and its variability. Measurements were compared with estimates of TL calculated from the Navy Standard Parabolic Equation (NSPE) acoustic model using a first guess geoacoustic bottom based on the literature. Other model inputs included bathymetry from the U.S. Coastal Relief Model, and sound speed profiles from Expendable Bathythermographs (XBT) and the Navy Coastal Ocean Model. Using data garnered from previous studies of the bottom sediment and sub-layer near the Southern California Offshore Range, variations of a geoacoustic model were constructed and input into the NSPE model. TL from all model runs were then analyzed across all frequencies to determine the best fit geoacoustic model to use with NSPE when applying it near SCORE for acoustic predictions. Research was funded by the United States Navy Chief of Naval Operations Environmental Readiness Division (CNO/N45).

14. SUBJECT TERMS Transmission Loss, Receive Level, Source Level, TL, RL, SL, Sound Exposure Model, Oceanography, NSPE, Tanner Bank, SCORE, SOAR, Parabolic Equation, Geoacoustic, Geoacoustic Inversion, Acousonde, G-34			**15. NUMBER OF PAGES** 59
			16. PRICE CODE
17. SECURITY CLASSIFICATION OF REPORT Unclassified	**18. SECURITY CLASSIFICATION OF THIS PAGE** Unclassified	**19. SECURITY CLASSIFICATION OF ABSTRACT** Unclassified	**20. LIMITATION OF ABSTRACT** UU

NSN 7540-01-280-5500 Standard Form 298 (Rev. 2-89)
Prescribed by ANSI Std. 239-18

THIS PAGE INTENTIONALLY LEFT BLANK

Approved for public release; distribution is unlimited

TUNING, VALIDATION, AND UNCERTAINTY ESTIMATES FOR A SOUND EXPOSURE MODEL

Francis J. Carmody
Lieutenant, United States Navy
B.S., University of Central Florida, 2000
M. Ed., University of Central Florida, 2001

Submitted in partial fulfillment of the
requirements for the degree of

MASTER OF SCIENCE IN PHYSICAL OCEANOGRAPHY

from the

NAVAL POSTGRADUATE SCHOOL
September 2011

Author: Francis J. Carmody

Approved by: John Joseph
Thesis Co-Advisor

Ching-Sang Chiu
Thesis Co-Advisor

Jeff Paduan
Chair, Department of Oceanography

THIS PAGE INTENTIONALLY LEFT BLANK

ABSTRACT

To tune and validate the performance of an acoustic model, sound signals were transmitted from a calibrated source, at varied mid-range frequencies. and received on a moored acoustic recording package at the edge of Tanner Bank near the Southern California Anti-Submarine Warfare Range (SOAR). The acoustic monitoring package was constructed of three calibrated Acousonde recorders. Source levels (SL) were measured at 1.8 meters from the source using a Bioacoustic Probe. Signals recorded on the Acousondes and the Bioacoustic Probe were processed to measure transmission loss (TL) and its variability. Measurements were compared with estimates of TL calculated from the Navy Standard Parabolic Equation (NSPE) acoustic model using a first guess geoacoustic bottom based on the literature. Other model inputs included bathymetry from the U.S. Coastal Relief Model, and sound speed profiles from Expendable Bathythermographs (XBT) and the Navy Coastal Ocean Model. Using data garnered from previous studies of the bottom sediment and sub-layer near the Southern California Offshore Range, variations of a geoacoustic model were constructed and input into the NSPE model. TL from all model runs were then analyzed across all frequencies to determine the best fit geoacoustic model to use with NSPE when applying it near SCORE for acoustic predictions. Research was funded by the United States Navy Chief of Naval Operations Environmental Readiness Division (CNO/N45).

THIS PAGE INTENTIONALLY LEFT BLANK

TABLE OF CONTENTS

I. INTRODUCTION....1
A. THESIS OBJECTIVES....1
B. THESIS APPROACH AND OUTLINE....1

II. EXPERIMENT DESIGN AND EXECUTION....3
A. ENVIRONMENTAL MODEL....3
1. Bathymetry and Sea Surface....3
2. Sound Speed Profiles....4
B. ACOUSTIC PATHS....7
C. ACOUSTIC SOURCE AND RECEIVER....8
D. NAVY STANDARD PARABOLIC EQUATION TRANSMISSION LOSS MODEL....13
E. GEOACOUSTIC INVERSION....13
F. GEOACOUSTICS....14

III. ANALYSIS....19
A. ACOUSTIC SIGNAL PROCESSING AND VARIABILITY....19
B. TUNING THE NSPE MODEL....22
1. Sediment Layer Variability for Tanner Bank....22
2. Sediment Layer Variability for the Slope of Tanner Bank....28
3. Rock Layer Variability....33

IV. CONCLUSIONS....35

IV. FUTURE RESEARCH....37
A. ANALYSIS OF OTHER DATA SETS....37
B. ANALYSIS OF OTHER AREAS....37

LIST OF REFERENCES....39

INITIAL DISTRIBUTION LIST....41

THIS PAGE INTENTIONALLY LEFT BLANK

LIST OF FIGURES

Figure 1. Southern California Offshore Anti-Submarine Warfare Range (SOAR) near San Clemente Island. Five acoustic paths were chosen emanating from a central receiver mooring. Dots along paths indicate the location of the transmission stations. (After Google Earth 2011).....2

Figure 2. Bathymetry near Tanner Bank. Red, green and yellow lines are the acoustic tracks. Black line is the edge of SOAR. The dots along the tracks are the transmission stations. (After Google Earth 2011). 3

Figure 3. Wind speed during transmissions, mean wind of 8.97 m/s.....4

Figure 4. XBT locations. The left figure shows a wide view. Contours are every 200 m. The right figure is a closer view with contours every 100 m in depth.....6

Figure 5. XBT and NCOM SSPs. The basic structure of the profiles is the same between the XBT and NCOM plots. The weaker gradient in the NCOM plots did not cause significant differences in model output.....6

Figure 6. (a) Bathymetry along the shallow path on Tanner Bank, (b) Bathymetry along the steep-slope path on the northeast slope of Tanner Bank. Source locations are in black, SSP locations are in red and bathymetry is in blue. Acousonde receivers are at 30, 60, and 90 meters deep at range = 0. 8

Figure 7. Type G-34 Projector. 9

Figure 8. Acousonde Receiver. Actual size measures 22.1 cm long, and 3.2 cm in diameter.....11

Figure 9. Mooring diagram. Designed and built by Marla Stone of NPS. Acousonde receivers are positioned at 30, 60, and 90 meters. Two SBE 39 pressure sensors are positioned at 45, and 75 meters. 12

Figure 10. Source locations. Figure (a) has 100 meters contours. Figure (b) has 200 meters contours. 15 source locations are at 6 meters deep. 8 source locations are at 50 meters in order to have broadcasts below the mixed layer. The Acousonde mooring is at 32.76 N, -119.22 W. 12

Figure 11. Spectrogram for one 5 minute transmission sequence. This transmission was from the final transmission made in the experiment. It is from a 250 meter range, 6 meter source depth, and 30 meter receiver depth. Dark red vertical lines indicate the 1-sec LFM sweeps. 19

Figure 12. TL variability. Red dots are calculated values for TL at 1 second intervals, and the blue is the trend line. This transmission was 200 meters from the mooring, at 6 meters deep and 2000 Hz. The Acousonde it was received on 30 meters deep. The TL for the entire 50 second period was 47dB. 20

Figure 13. Top Left – San Nicholas Island Buoy, Bottom Right – San Clemente Island Buoy, Bottom Left – Tanner Basin Buoy (not reporting wave data), (After Google Earth 2011). 21

Figure 14. a) Standard Deviation above TL. 81% of the 345 received signals had an upper bound for standard deviation of 6dB. b) Standard Deviation below

TL. 93% of the 345 received signals had a lower bound for standard deviation of 3dB. 21
Figure 15. Full field TL plot of the shallow region of Tanner Bank. The heavy black line is the sea floor. The illustration shows the extent of sound penetration into the sediment layer. Source locations are black circles at 6 meter and 50 meter depths. The Acousonde receiver mooring is at the range of 0 km on the left side of the figure. 26
Figure 16. While all of the models have the same trends, minus the mud model with a few deviations, the geoacoustic model with the coarsest grain size yields results closest to observed TL. 26
Figure 17. With similar results to the receiver at the 30 meter depth, the receiver at the 60 m depth shows that the best results of modeled TL come from the geoacoustic model using Bachman's equations with the coarsest grain size. 27
Figure 18. On the bottom receiver, at a depth of 90 meters, the coarsest grain size of 1.152 φ almost comes within one standard deviation a every sampled range. 27
Figure 19. Full field TL plot of the sloping region of Tanner Bank. The heavy black line is the sea floor. The illustration shows that with fewer bottom interactions than on Tanner Bank itself, there is a lesser extent of sound penetration into the sediment layer. Source locations are black circles at 6 meter and 50 meter depths. The Acousonde receiver mooring is at the range of 0 km on the left side of the figure. 31
Figure 20. The top receiver, 30 meters deep, along the slope, shows little difference between geoacoustic models, with the exception of the mud bottom, which gets worse with increased range. 31
Figure 21. The coarse grain size of 2.828 φ, and Bucca's fine sand model are consistent with each other and statistically produce results of modeled TL closest to observed TL. 32
Figure 22. This illustration of the modeled TL to the bottom receiver at 90 meters deep, along the slope, shows why the fine grain size, 5.724 φ, model does not statistically perform well. For the 5.724 φ curve, a large fluctuation occurs at 1.5 km, with smaller yet noticeable deviations at 4.5, and 5.5 km. 32

LIST OF TABLES

Table 1. Frequencies and source levels from the G-34. 10

Table 2. Values used for the geoacoustic model presented by Bucca and Fulford (1995). The variable z is the depth below the sea floor in meters. 23

Table 3. Statistical results for the shallow leg geoacoustic models. All results shown are for a thickness of 4 meters, which provided the best results when comparing thickness. The trend of better results by using smaller φ values is apparent. 25

Table 4. Statistical results for the sloping leg. All results shown are for a sediment thickness of 75 meters, which provided the best results when comparing statistics across thickness values holding grain size constant. The more coarse grain sizes provide the best statistics, although there is not one-grain size that dominates across all statistics. 30

THIS PAGE INTENTIONALLY LEFT BLANK

LIST OF ACRONYMS AND ABBREVIATIONS

ASW	Anti-Submarine Warfare
CW	Continuous Wave
CTD	Conductivity Temperature Depth system
DBDB-V	Digital Bathymetry Data Base - Variable Resolution
HARP	High Frequency Acoustic Recording Package
LFM	Low Frequency Modulation
NCOM	Navy Coastal Ocean Model
NSPE	Navy Standard Parabolic Equation model
NUWC	Naval Undersea Warfare Center
PC-IMAT	Personal Computer Interactive Multi-Sensor Analysis Training Tool
RAM	Range-dependent Acoustic Model
RL	Receive Level
RMS	Root Mean Square
SCORE	Southern California Offshore Range
SOAR	Southern California ASW Range
SOCAL BRS	Southern California Behavioral Response Study
SONAR	Sound Navigation and Ranging
SSFPE	Split-Step Fourier Parabolic Equation
SSP	Sound Speed Profile
SSPPE	Split-Step Padé Parabolic Equation
STDA	Sonar Tactical Decision Aid
TL	Transmission Loss
TVR	Transmit Voltage Response

USWTR	Undersea Warfare Training Range
XBT	Expendable Bathythermograph

ACKNOWLEDGMENTS

The author would like to acknowledge the support of the Chief of Naval Operations Environmental Readiness Division, (CNO/N45), for the funding of this experiment.

I would also like to thank Commander John Joseph (Retired) for his dedication to this project. His tireless efforts made this entire project possible. I would like to thank Mr. Chris Miller and Professor Ching-Sang Chiu for their efforts. If not for their insight and forethought, I would not have been able to do this. To Marla Stone, I say thank you for creating our mooring and risking her life with us aboard the R/V Sproul while conducting the field research.

To my dear wife, Denice, I say thank you for sticking by my side for 17 years, every one of them better than the last. If not for her support, I would not be the man I am today. I look forward to many more years with her. I only wish I could support her as much as she supports me. Thank you. My sons, Frankie and Kyle, also deserve much of my gratitude for their patience and understanding during this process. I wish that I had more time to spend with them, but I hope they can see that hard work and dedication pay off.

THIS PAGE INTENTIONALLY LEFT BLANK

I. INTRODUCTION

A. THESIS OBJECTIVES

The objective of this thesis is to support Navy Anti-Submarine Warfare (ASW) training activities in the eastern Pacific by validating and tuning an acoustic model that can be used as the basis for estimating sound exposure levels from mid-frequency SONAR, and by providing uncertainty estimates for the model output. The tuned acoustic model can be used by the Southern California Marine Mammal Behavioral Response Study (SOCAL BRS), and operators of the Sonar Tactical Decision Aid (STDA), and the Personal Computer Interactive Multi-Sensor Analysis (PC-IMAT) training tool.

B. THESIS APPROACH AND OUTLINE

The motivation for this thesis came from a desire to improve ASW training and operations. The region of the Pacific to be modeled was chosen as the western edge of the Southern California Anti-Submarine Warfare Range (SOAR) (shown in Figure 1), which is part of the Southern California Offshore Range (SCORE). Specifically, an acoustic path over the shallow region of Tanner Bank and a second steep slope path extending from Tanner Bank towards a bottom mounted High Frequency Acoustic Recording Package (HARP) located at 32.8469 N, -119.1767 W, deployed by Scripps Institution of Oceanography. This location provided for the analysis of the model over two distinct topographies, as well as the ability to further tune and validate the model after the recovery of data from the HARP and hydrophones located on the seafloor at the western edge of SOAR.

Preliminary model runs were conducted to verify that transmission loss (TL) measurements at desired ranges were achievable. An acoustic source—a Type G-34 Projector—was used. The G-34 transmitted mid-frequency signals off the side of the R/V Robert Gordon Sproul, while on a research cruise in conjunction with Scripps Institute of Oceanography, from 09–12May2011. Fifteen stations were chosen for transmissions using two source depths. Five mid-range frequencies, 1–5 kHz at 1 kHz

intervals, were transmitted at each location, approximately 1.5–2 km apart. An acoustic receiver array was built using three calibrated Acousonde recording devices, commonly used as whale tags, and two Seabird temperature/pressure sensors to verify depth. Recorded acoustic data were recovered and processed for TL measurements between the source and receiver. Observed TL was then compared with TL estimates calculated from the Navy Standard Parabolic Equation (NSPE) model. Systematic changes were made to the geoacoustic model in order to test NSPE's sensitivity to geoacoustics. Analysis of the observed TL versus modeled TL was done to measure uncertainty, and to arrive at recommendations for the best geoacoustic model to be used when modeling acoustic propagation in the vicinity of Tanner Bank.

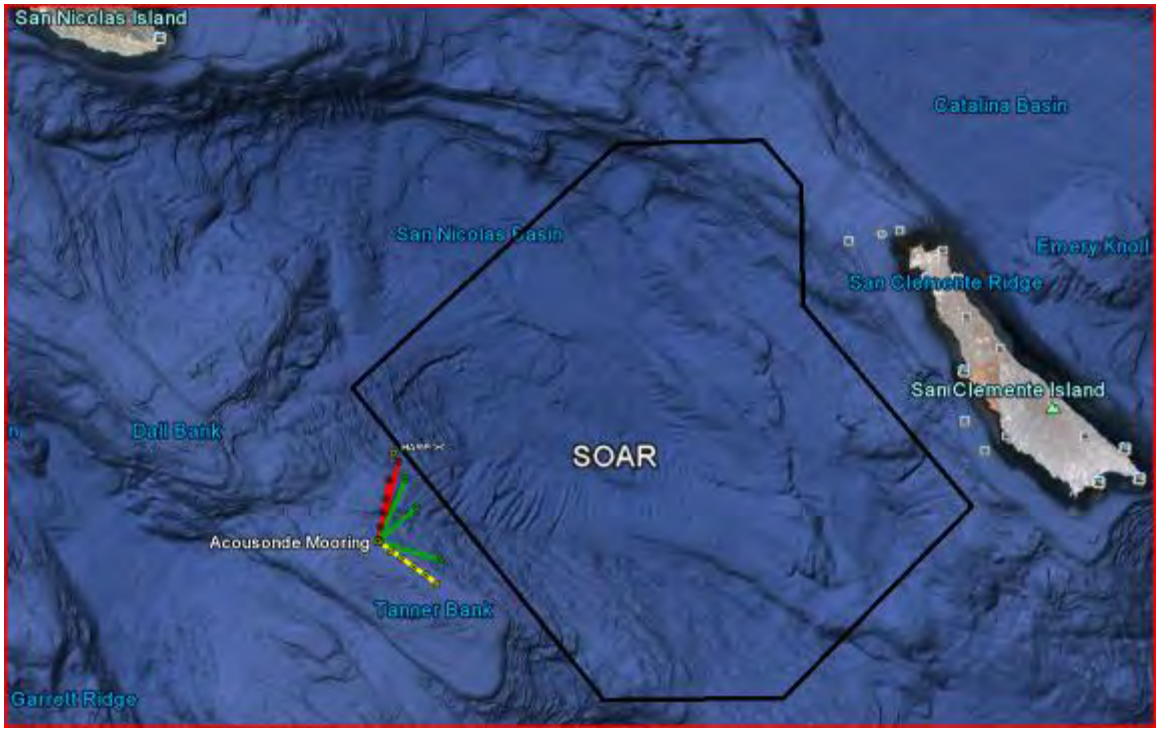

Figure 1. Southern California Offshore Anti-Submarine Warfare Range (SOAR) near San Clemente Island. Five acoustic paths were chosen emanating from a central receiver mooring. Dots along paths indicate the location of the transmission stations. (After Google Earth 2011).

II. EXPERIMENT DESIGN AND EXECUTION

A. ENVIRONMENTAL MODEL

1. Bathymetry and Sea Surface

Bathymetry data was added to the NSPE model from the 3 arc-second U.S. Coastal Relief Model, which is the same model used by the U.S. Navy's Digital Bathymetric Data Base Variable Resolution (DBDB-V)**.** Figure 2 shows the bathymetry of the region where the experiment was conducted. The bathymetry data were interpolated to points along the modeled paths at the same resolution provided by the database.

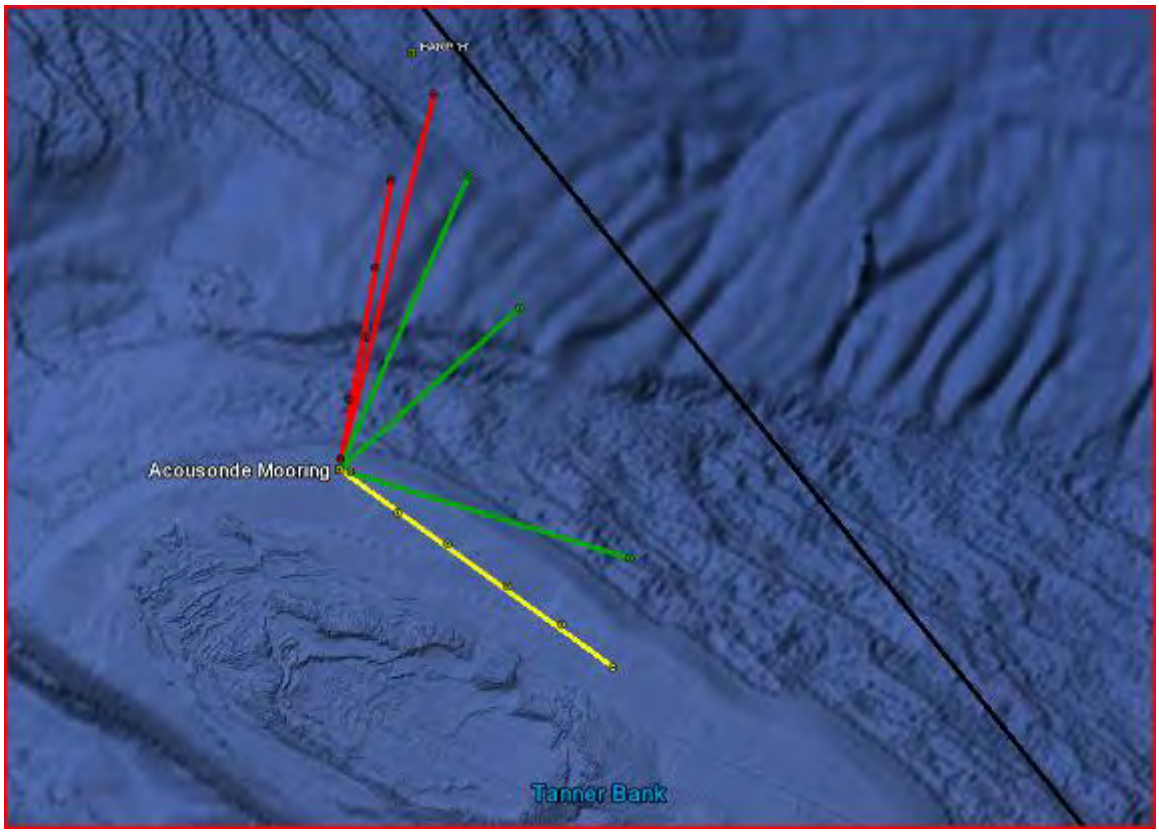

Figure 2. Bathymetry near Tanner Bank. Red, green and yellow lines are the acoustic tracks. Black line is the edge of SOAR. The dots along the tracks are the transmission stations. (After Google Earth 2011).

Scattering losses at the sea surface were accounted for with wind speed data collected aboard the R/V Sproul. The wind speed throughout the evolution was moderately strong with a mean value of 8.97 m/s and a standard deviation of 1.82 m/s. The NSPE model uses surface wind as a basis to account for surface scattering losses.

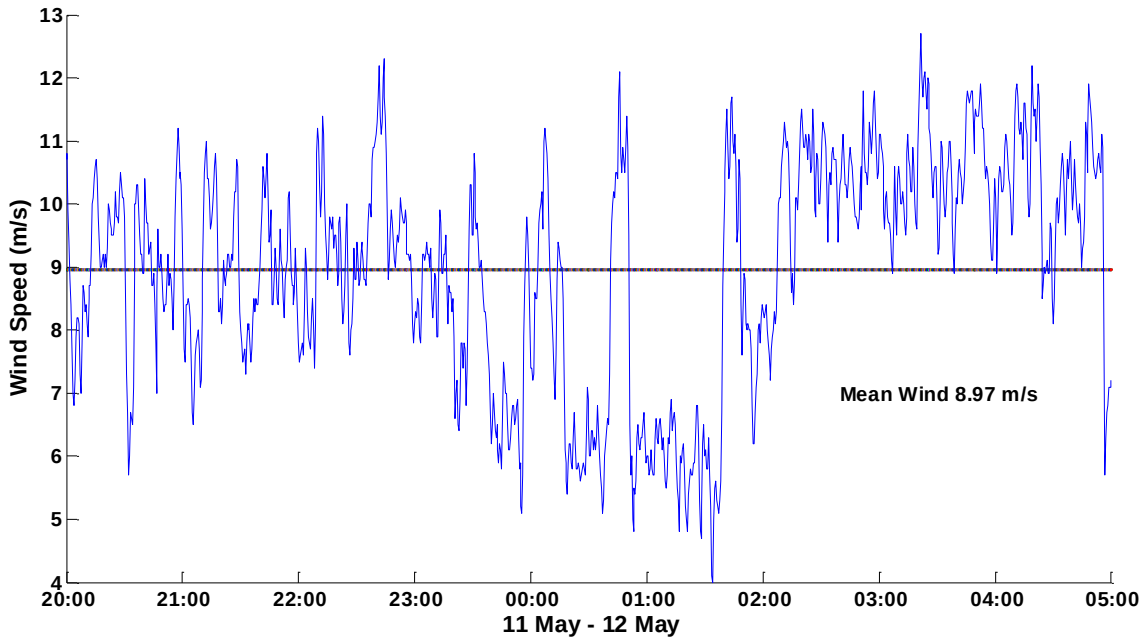

Figure 3. Wind speed during transmissions, mean wind of 8.97 m/s.

2. Sound Speed Profiles

Sound speed profiles (SSP) were input into the NSPE model using data collected from Sippican T4, T6, and T7 Expendable Bathythermographs (XBT). The U.S. Navy Coastal Ocean Model (NCOM) salinity and temperature values were also used as inputs into the SSPs. NCOM for the Southern California region is a 3-km resolution model. All three XBT types have a depth accuracy of ±4.6 meters, a vertical resolution of 0.65 meters and a temperature accuracy of $\pm 0.1^{o}$ C. The T4 and the T6 are rated at 460 meters and the T7 is rated at 760 meters (Lockheed Martin Maritime Systems and Sensors 2005). The NCOM data were retrieved from the NCOM model run for the nearest date and forecast time for each transmission.

NCOM predicted temperature, depth and salinity were combined using the Mackenzie equation (Equation 2.1) for calculating sound speed to create SSPs along the

acoustic tracks at 1-km increments. The NCOM SSP was created at depth increments of those provided by NCOM, which begins at 2-meter increments increasing with depth to 100-meter increments at 1000 meters.

$$c = 1448.96 + 4.591T - 5.304\times10^{-2}T^2 + 2.374\times10^{-4}T^3 + 1.340(S-35) + 1.630\times10^{-2}D + 1.675\times10^{-7}D^2 - 1.025\times10^{-2}T(S-35) - 7.139\times10^{-13}TD^3 \quad (2.1)$$

T = temperature in degrees Celcius
S = salinity in parts per thousand
D = depth in meters

XBTs were launched at each position where the source signal was transmitted (Figure 4). XBTs collected accurate temperature versus depth measurements that were then combined with NCOM salinity predictions to create SSPs at the positions shown in Figure 5 using the Mackenzie equation. One T5 XBT that is rated to a depth of 1830 meters was used at an earlier time of the day to obtain deep-water values. A CTD was planned to have been launched, but was not conducted. Rough seas throughout the cruise had been putting us behind schedule. Conducting our scheduled transmissions, were more important than launching the CTD.

In the XBT data, a mixed layer was observed to depths ranging from 7–20 meters. The maximum depth of the mixed layer for the NCOM data is within 3 meters of the XBT SSPs. The main thermocline existed from the bottom of the mixed layer to depths ranging from approximately 40–65 meters. As seen from Figure 5, it is evident that the basic structure of the SSPs for both NCOM and XBT data is the same, with the XBT showing a stronger gradient. This is evidence of a cooler water mass in the 50–100 meter depths than forecast by NCOM. Seven acoustic model runs were performed, using both XBT and NCOM SSPs with various geoacoustic parameters. The parameters were set to the extreme ends of the geoacoustic input envelopes (to be discussed later), with little difference noted in the TL output. It is expected that SSPs created from NCOM would provide sufficient realism when little data are available; however, only XBT SSPs were used for model tuning, since these are expected to show a truer representation of the

environment. Given the strong downward refracting environment, only short direct paths existed. This speaks to the need for the geoacoustic tuning in shallow environment areas where significant bottom interaction is expected.

a) b)

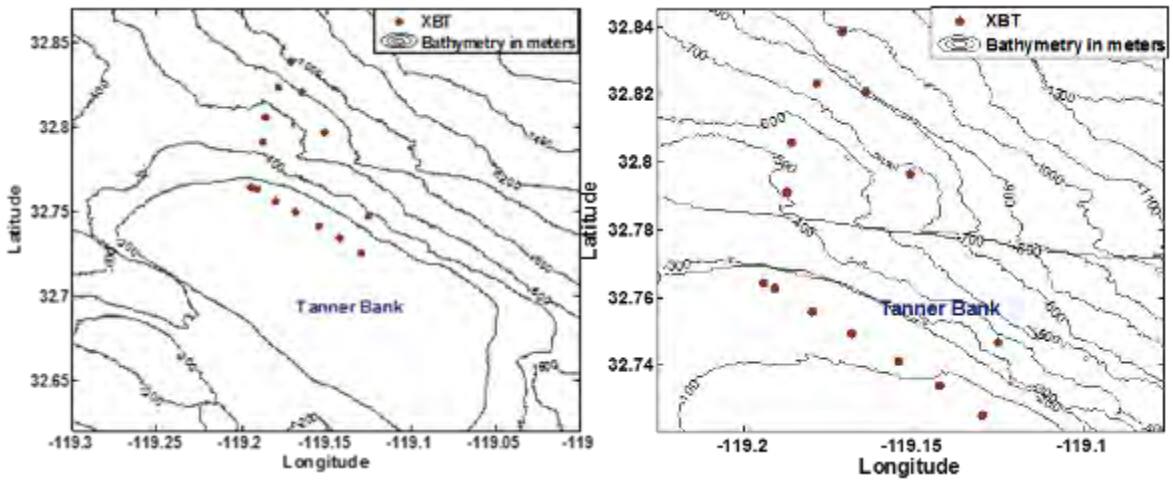

Figure 4. XBT locations. The left figure shows a wide view. Contours are every 200 m. The right figure is a closer view with contours every 100 m in depth.

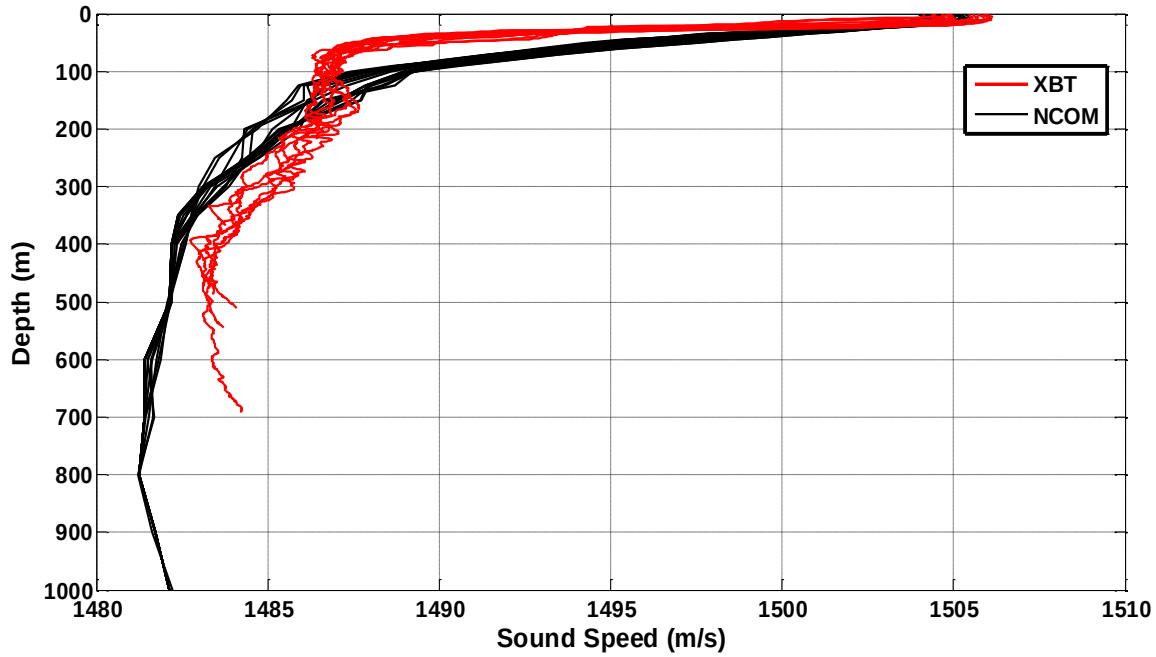

Figure 5. XBT and NCOM SSPs. The basic structure of the profiles is the same between the XBT and NCOM plots. The weaker gradient in the NCOM plots did not cause significant differences in model output.

B. ACOUSTIC PATHS

The primary acoustic paths analyzed in this study were: 1) the southern path along the edge of Tanner Bank (Figure 2, yellow, and, 2) the western path from the Acousonde mooring in the direction of the HARP (Figure 2, red). TL along the three paths in the middle (Figure 2, green), were modeled in an effort to maximize data collection at other receivers of opportunity for later analysis.

The acoustic path along Tanner Bank went from 32.725^{o} N, -119.130^{o} W to the Acousonde mooring and was labeled the yellow path. The depth of this path was 128 meters at the mooring with a gentle upslope to 90 meters at 7.4 km southeast of the mooring. The bathymetry along this path and source locations are shown in Figure 6a. This path was chosen to model a shallow region as it presents an environment with high bottom interaction.

The acoustic path from the Acousonde mooring to the HARP was labeled as the red path. This path is on the slope of Tanner bank, beginning with a depth of approximately 128 meters extending downward to a depth of approximately 995 meters at 8.5 km from the mooring. The bathymetry of this path as well as the source locations used can be seen in Figure 6b. This path was chosen for its steep slope environment.

The three paths labeled in green were decided upon with the anticipation of recovering and analyzing data from the HARP and bottom mounted range hydrophones at the western edge of SOAR. Each of these three tracks has only one transmission location at ranges of approximately 8.5–5.3 km as depicted in Figure 2. Data from these paths were included in the analysis of the red paths as they have similar steep slope acoustic environments.

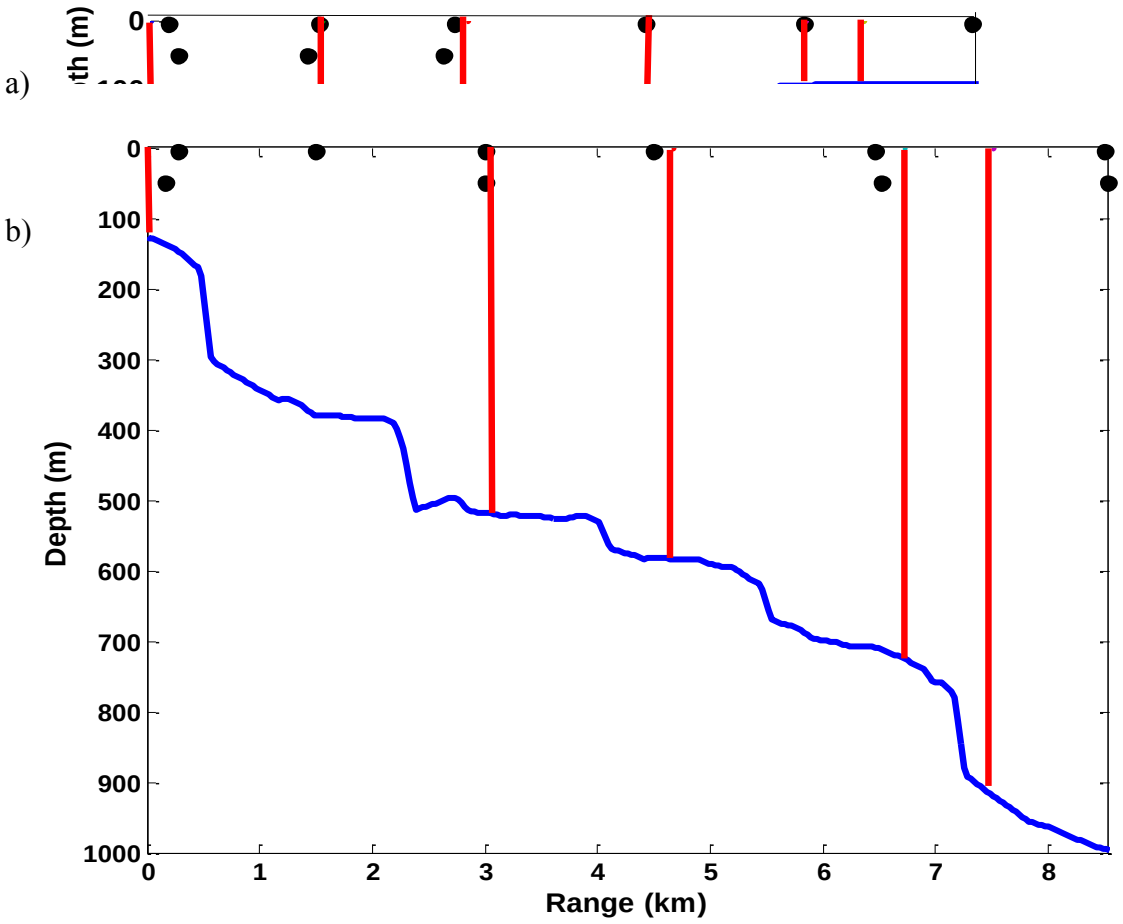

Figure 6. (a) Bathymetry along the shallow path on Tanner Bank, (b) Bathymetry along the steep-slope path on the northeast slope of Tanner Bank. Source locations are in black, SSP locations are in red and bathymetry is in blue. Acousonde receivers are at 30, 60, and 90 meters deep at range = 0.

C. ACOUSTIC SOURCE AND RECEIVER

The sound source, a Type G-34 Projector, was chosen for its ability to transmit in the mid-frequency band, typical of Navy active SONAR. The projector has a frequency range of 200–5,000 Hz with a maximum operational depth of 1379 meters. It can be driven at up to 1,000 Volts (Naval Undersea Warfare Center 2011). The source was calibrated by the Naval Undersea Warfare Center (NUWC).

Figure 7. Type G-34 Projector.

Calibrated CW tonals from 1–5 kHz were generated and broadcast at depths of 6 and 50 meters. For the purpose of measuring source level (SL), a calibrated acoustic recorder, the Bioacoustic Probe, was placed 1.8 meters above the source for the duration of the experiment. Its pressure field was processed at 1, 2, and 3 kHz, frequencies. SLs for the 4 and 5 kHz signals could not be accurately measured by the Bioacoustic Probe due to the instrument's sampling rate ($f_s \approx 10{,}000$Hz). To calculate the SL at the 4 and 5 kHz frequencies, near field data from the receiver mooring was used in conjunction with the Bioacoustic Probe calculations. All frequencies and SLs are in Table 1.

Frequency (kHz)	Source Level (dB)
1	149.9
2	162.9
3	173.4
4	173.4
5	173.4

Table 1. Frequencies and source levels from the G-34.

As a calibrated reference transducer, G-34 SLs can be calculated using a provided Transmitting Voltage Response (TVR) curve with measured input voltages. Aboard the R/V Sproul, the winch wire has a central conducting wire used to connect the amplifier to the source. This allowed the source to be independently lowered to any depth. The coiling of a 5,000 meter wire created a frequency dependent inductive effect on the voltage seen by the G-34. Due to our inability to measure the true voltage at the source we were unable to apply the TVR curve for source level measurement.

The source was lowered to depths at which typical hull mounted active SONAR might be located, specifically 6 meters. A 50-meter source depth was chosen to obtain measurements from below the surface layer. Source locations were predetermined to be at 1.5–2 km intervals (Figure 10); variability is due to ship drift during the transmission. During each transmission, the source was lowered over the side of the vessel as the vessel attempted to maintain station in rough seas. Tones at frequencies 1, 2, 3, 4, and 5 kHz were transmitted. Each continuous wave (CW) frequency was broadcast for 55 seconds with a 1-second linear frequency modulation (LFM) sweep in between to use as markers. Twenty one seconds of 1-second LFM sweeps were also broadcast to aid in identifying the beginning of each transmission period.

The receiver mooring was designed using Acousonde recorders. The Acousonde, developed by Dr. William Burgess of Greeneridge Sciences Inc. is a 22.1 cm long, 9.2

ounce autonomous recorder capable of a maximum operating depth of 3000 meters and a maximum continuous sampling rate of 232 kHz. The three Acousondes used in this experiment were set to a sampling rate of 29,038 Hz, with an anti-aliasing cutoff frequency of 9,292 Hz. They were positioned on a mooring to be at water depths of 30 m, 60 m, and 90 m (Figure 9). The predecessor to the Acousonde, a Bioacoustic Probe, was positioned 1.8 meters above the G-34 source to aid in establishing SLs (Greeneridge Sciences 2011).

Figure 8. Acousonde Receiver. Actual size measures 22.1 cm long, and 3.2 cm in diameter.

The Acousonde mooring was deployed at a 128 meter water depth. The depths of the Acousondes were verified by two Seabird SBE 39 Temperature/Pressure Sensors. The sensors were moored at 45 and 75 meters, respectively, and the final depth of the Acousondes was determined by reference to the actual depth of the pressure sensors (Figure 9). After recovery and conversion from pressure to depth using Saunders' method, it was determined that each Acousonde was only 0.5 m shallower than planned. The Saunder's pressure to depth conversion is:

$$z = (1 - c_1)p - c_2 p^2$$

where

$$c_1 = (5.92 + 5.25\sin^2\varphi) \times 10^{-3} \ {}^{m}/_{dbar} \text{ with } \varphi = \text{ latitude in degrees} \qquad (2.2)$$

$$c_2 = 2.21 \times 10^{-6} \ {}^{m}/_{dbar^2}$$

and assuming a standard ocean Temperature = $0°C$, Salinity = 35 NSU

The position of the mooring was verified by acoustic ranging to determine the location of the anchor.

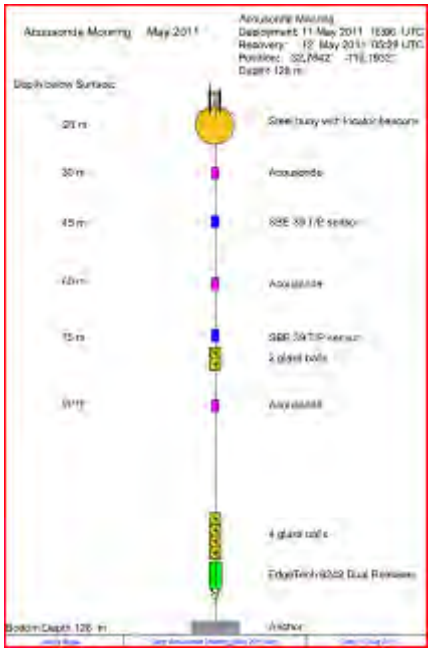

Figure 9. Mooring diagram. Designed and built by Marla Stone of NPS. Acousonde receivers are positioned at 30, 60, and 90 meters. Two SBE 39 pressure sensors are positioned at 45, and 75 meters.

a) b)

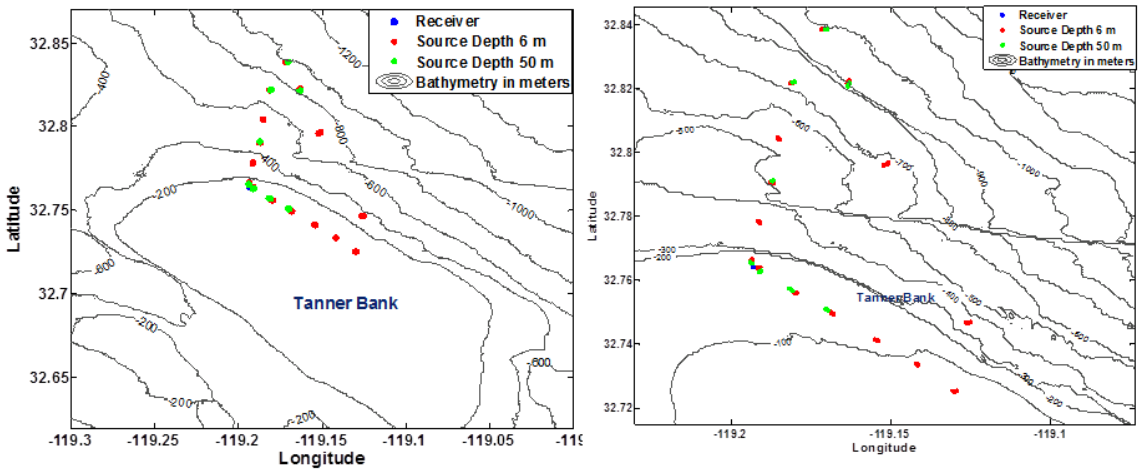

Figure 10. Source locations. Figure (a) has 100 meters contours. Figure (b) has 200 meters contours. 15 source locations are at 6 meters deep. 8 source locations are at 50 meters in order to have broadcasts below the mixed layer. The Acousonde mooring is at 32.76 N, -119.22 W.

D. NAVY STANDARD PARABOLIC EQUATION TRANSMISSION LOSS MODEL

The Navy Standard Parabolic Equation (NSPE) model consists of two methods of solving the acoustic parabolic wave equation. The first method is the Split-step Fourier PE (SSFPE) and the second is the newer Split-Step Padé PE (SSPPE), also known as the Range-dependent Acoustic Model (RAM), developed by Michael Collins of the Navy Research Laboratory. RAM is an improved version of a finite element split-step model and ―has been shown to produce significantly more accurate results than SSFPE" in environments with significant bottom interaction such as the case with Tanner Bank (Naval Oceanographic Office 2009).

RAM is valid for problems with high angle propagation and large depth variation. It was developed to be as accurate as higher order PE solutions, yet two-orders of magnitude faster than finite difference solutions (Collins 1992). Padé approximations account for both asymptotic and numerical accuracy, which is how a greater efficiency is achieved. When used on a computer with multiple processors, ―each processor performs the equivalent of a single step in the finite difference PE algorithm for the wide–angle PE" (Collins, 1994). The output of each processor is then combined in a single solution.

The user provides NSPE with an input file containing relevant environmental parameters. These parameters consist of source depth, frequency, and receiver depth. Environmental data such as wind speed, to account for scattering losses at the surface, and sound speed profiles are also input, as well as bathymetry, and geoacoustic information. The geoacoustic model includes thickness of sediment layers, bottom density, compressional sound speed and attenuation, shear sound speed and attenuation, and information about secondary layers. The model allows these factors to be changed based on range and depth. TL as a function of range is derived from the complex pressure field calculated by the model (Naval Oceanographic Office 2009)

E. GEOACOUSTIC INVERSION

A geoacoustic inversion is any method by which the properties of the sea floor are accurately estimated by establishing a geoacoustic model based on measurements and

validating that model with acoustic measurements (Larsen 2006). Hamilton's definition of the geoacoustic model is that "of the real sea floor with emphasis on measured, extrapolated, and predicted values of those properties important in underwater acoustics and those aspects of geophysics involving sound transmission" (1980).

Due to the nature of the "invariably insufficient" data available on the sea floor, the geoacoustic modeler must make predictions "based on extrapolations from similar areas and sediment types" (Hamilton 1980). After developing a geoacoustic model, its final interpretation should be based off of the "benefit of knowledge of … measured transmission loss data" (Bucca 1994).

F. GEOACOUSTICS

The geoacoustic models input to NSPE were based on the research of J. E. Holzman, "Submarine Geology of Cortes and Tanner Banks" (1992), R. T. Bachman, "A Three-Dimensional Geoacoustic Model for the Catalina Basin" (1994), and Paul J. Bucca with James K. Fulford, "Environmental Variability During the Tanner Bank Phase of the Pacific Coast Operation", (1995). The methods of Hamilton (1980) were studied and implemented to the extent possible. The sediment and rock types were defined; thickness of the layer was established. Compressional wave speeds and attenuation factors were calculated along with shear wave speeds and attenuation factors. Finally, values for sediment and rock densities were determined. Each researcher provided different information with which to hypothesize the best geoacoustic model for the region.

Bachman's study is based on the Catalina Basin, just on the other side of San Clemente Island from Tanner Bank and San Nicholas Basin. Bachman proposed a suite of equations to calculate sound speed, density, and sound attenuation based on previous work by Hamilton (1985), Hamilton (1976), and Bachman (1985) are valid for the Catalina Basin. The equations determine the values for the properties base on sediment grain size and sediment thickness. He distinguishes between fine sediments as being greater than 4.5 φ and coarse sediments as being less than 4.5 φ, where $\varphi = -\log_2(\text{grain size in mm})$. Sediment thickness from Bachman's research was hypothesized to be up to 3 meters on the tops of ridges. Tanner Bank, being similar to a

ridge in the Catalina Basin, should have a very shallow sediment thickness. The sediment thickness in the deeper regions on the slope of Tanner Bank is hypothesized to be approximately 160 meters deep. It is based on a two-way travel time measurements of 0.2 seconds from a similarly deep spot in the Catalina Basin on Figure C-1 of Bachman's paper, and his example calculation with the same two way travel time. Sediment grain size estimations of 5 φ on the slope of Tanner bank and 3 φ on Tanner Bank are based on similar locations from Catalina basin chosen from Bachman's Figure E-1. The underlying bedrock of the Tanner Bank area was hypothesized to be Mio-Pliocene sedimentary rock based on the location of the Catalina Basin in relation to San Nicholas Basin and rock types identified in Figure 3 of Bachman's paper. This gives values for compressional wave speed in the rock of 2300 m/s, density of 2.21 g/cm^3, and a compressional attenuation factor of 0.009 dB/m/kHz.

In the 1952 paper "Submarine Geology of Cortes and Tanner Banks," J. Holzman reveals information from his study of 66 bottom samples of the region. According to Holzman, the grain size distribution of the sediment in the region is due to "the material available and the subsequent working of the sediments by current activity." On the more shallow areas atop the bank, ample food is available for benthonic organisms. It is the decay of dead benthonic organisms that leads to coarse sediment. Fine sediments in the shallows are winnowed by the current onto the slopes. Grain sizes used to build a geoacoustic model were taken from Table III and Plate 5 of the paper. Mean grain sizes of 0.5–0.25 mm on the bank were used corresponding to 0.69–1.38 φ. On the slope mean grain sizes of 0.25–0.125 mm corresponding to 1.38–2.08 φ, respectively.

The Pacific Coast Operation, a multi-laboratory acoustic field measurement program that took place in 1994 with a major phase near the Tanner Bank, made several conclusions, which were used in building a geoacoustic model. According to Bucca and Fulford the "primary determinant for the acoustic response of the seafloor is the depth to which the sediments extend and not the sediment type or grain size" (1994). From their research they hypothesized the depth of the sediment on Tanner Bank to have a maximum thickness of 6 meters and found other data sets that suggest the thickness is highly variable and in some places nonexistent. Most of the acoustic energy

encountering the bottom is reflected back into the water column making the influence of the grain size nearly irrelevant. Based on 9 sediment grabs, grain size was determined to be commensurate with Holzman's research. Bucca and Fulford proposed two geoacoustic models for the area. For fine sand a compressional speed of 1700 m/s, compressional attenuation of 0.35 dB/m/kHz and a density of 1.7 g/cm^3, all extending to 6 meters below the ocean bottom. For mud, a depth dependent compressional speed of 1470 + 1.33m/s per meter below the bottom, compressional attenuation of 0.06 dB/m/kHz and a density of 1.5 g/cm^3 were proposed. Below the sediment layer in the sandstone a compressional speed of 2500 m/s, a compressional attenuation of 0.03 dB/m/kHz, and a density of 2.2 g/cm^3 were proposed.

The preceding three studies were used to generate the parameters for the geoacoustic model. The end parameters studied were compressional sound speed in the sediment, compressional attenuation in the sediment, thickness of the sediment, density of the sediment, compressional sound speed in the underlying rock layer, and compressional attenuation in the underlying rock. Only one value for density in the underlying rock layer was found in the literature therefore it was held constant at that value for this study. The input variables were sediment grain size and sediment depth since the compressional sound speed and attenuation are based on depth, and density is based on grain size as presented in Bachman (1995). In the cases from Bucca and Fulford, where the values for compressional sound speed, attenuation, and density were given, those values were input directly.

The ranges and increments of grain size and sediment thickness used to vary the geoacoustic model were based on the values presented in the literature. Each parameter was studied by varying the one in question, while holding the others constant. Having up to 8 increments for each parameter and 345 sound transmissions to compare, nearly 15,000 model runs were completed. More than 95,000 calculations of modeled TL were available for statistical comparison with observed values to determine efficient geoacoustic model.

For the grain size parameter, on Tanner Bank, it was varied from 0.69–3.462 φ at an increment of 0.462 φ. On the slope, the grain size was varied from 1.38–5.724 φ at an

increment of 0.724 φ. The grain size parameters were based on Bachman and Holzman's work. For the cases where grain size was not analyzed, values for compressional sound speed and attenuation, shear sound speed and attenuation, and density from Bucca and Fulford were used in the model. It is important to note that for the Bucca and Fulford geoacoustic model there are no parameters that have thickness dependence.

For sediment thickness on Tanner Bank, the parameter was varied from 0–6 meters at an increment of 1-meter. For the slope, the sediment thickness parameter was varied from 75–225 meters at an increment of 25 meters.

For the underlying rock layer, a density of 2.21 g/cm^3 was used. Based on a compressional sound speed ranging from 2300–2500 m/s, which was incremented at 30 m/s, a compressional attenuation of 0.0207–0.0225 dB/m/kHz was input using Bachman's equation.

THIS PAGE LEFT INTENTIONALLY BLANK

III. ANALYSIS

A. ACOUSTIC SIGNAL PROCESSING AND VARIABILITY

A total of 115 CW acoustic transmissions were broadcast and collected on three Acousonde receivers. Each broadcast was a 55-second CW signal at each of five frequencies. Signals were identified within the receive data by analyzing spectrograms of relevant time periods. To ensure only CW transmitted signal was processed, the middle 50 seconds were used for analysis. Each transmission was filtered using a 4th order Butterworth filter with a 10 Hz band around the center frequency. TL values were calculated from the differences of the SL and the RL of the broadcast. RLs were based on root mean square (RMS) pressure for 50 seconds. A spectrogram of a typical broadcast sequence is shown in Figure 11.

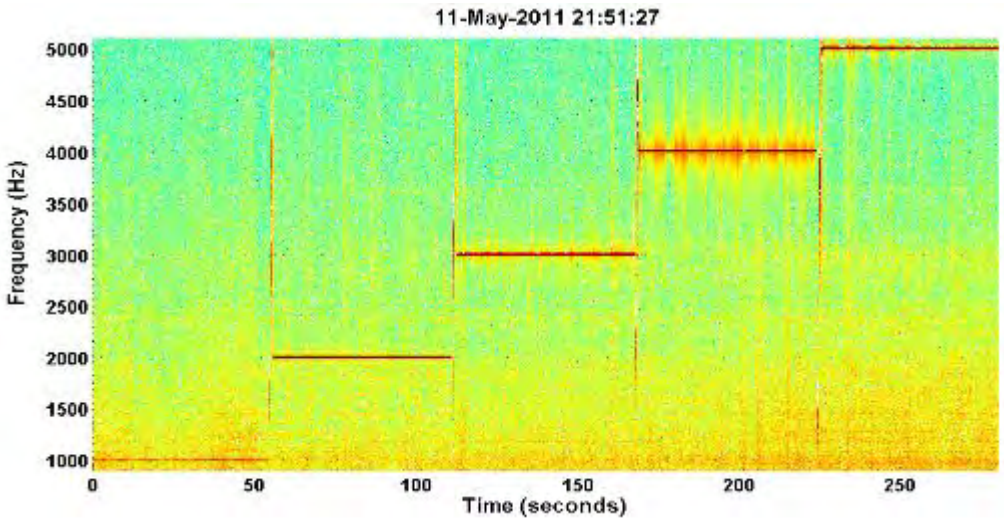

Figure 11. Spectrogram for one 5 minute transmission sequence. This transmission was from the final transmission made in the experiment. It is from a 250 meter range, 6 meter source depth, and 30 meter receiver depth. Dark red vertical lines indicate the 1-sec LFM sweeps.

To investigate variability and uncertainty in the observed TL measurements, each transmission was also analyzed as fifty, 1-second segments with a TL calculated for each segment. These fifty TL values fluctuated with time as can be seen in Figure 12, which is indicative of the variability that occurred within a 50 second segment. The mean period

of the fluctuations was calculated to be 5 seconds, which may be accounted for by the continuous change in water depth of approximately 2-m due to swell height. This phenomenon is described in ~~–O~~bservations of Fluctuation of Transmitted Sound in Shallow Water" (Urick 1969). Mean wave periods from the San Clemente Island Buoy and the San Nicolas Island Buoy, were 5.61 and 5.96 seconds, at 82 and 113 km from the receiver, respectively. Figure 13 shows the location of buoys from which data was used.

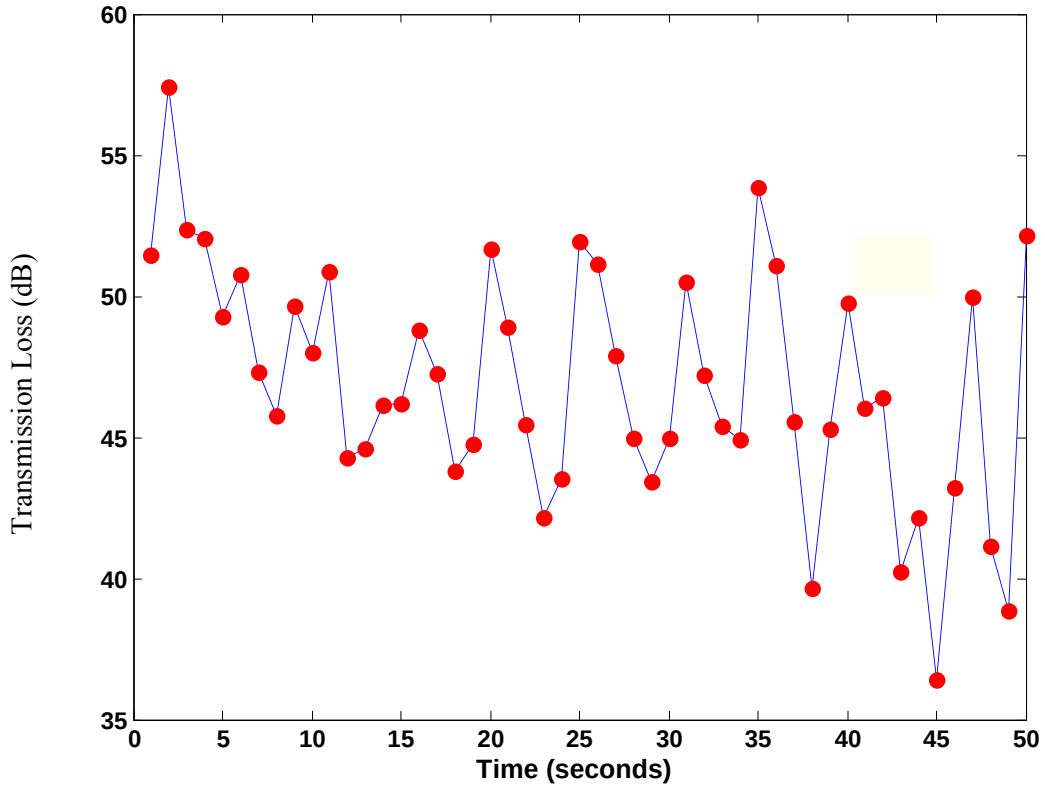

Figure 12. TL variability. Red dots are calculated values for TL at 1 second intervals, and the blue is the trend line. This transmission was 200 meters from the mooring, at 6 meters deep and 2000 Hz. The Acousonde it was received on 30 meters deep. The TL for the entire 50 second period was 47dB.

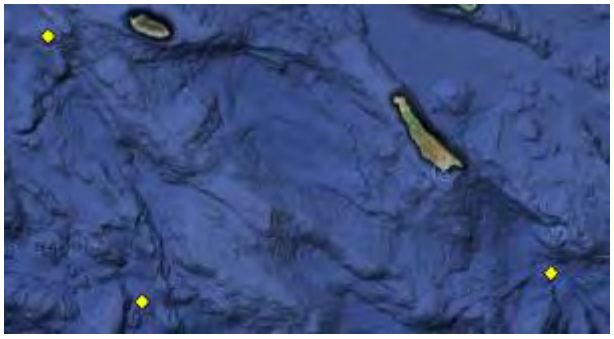

Figure 13. Top Left – San Nicholas Island Buoy, Bottom Right – San Clemente Island Buoy, Bottom Left – Tanner Basin Buoy (not reporting wave data), (After Google Earth 2011).

A standard deviation for transmission loss was calculated from the standard deviation of the RMS pressure for each 50 second transmission. Due to TL being on a log scale, the standard deviation below the mean is less than the standard deviation above the mean after conversion to dB from pressure. Since the received pressure changes with range and depth, a standard deviation was calculated for each of the 345, fifty second transmissions. Greater than 93% of the standard deviations were found to be within 4 dB below the mean TL, and greater than 81% were found to be within 6 dB above the mean TL. Histograms of the standard deviations from mean transmission loss for each of the 345 collected transmissions are shown in Figure 14.

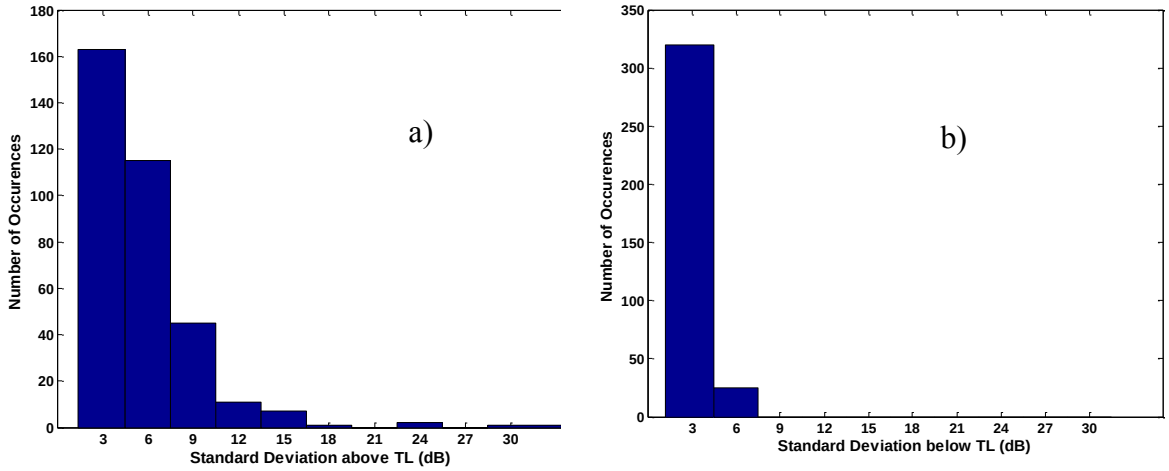

Figure 14. a) Standard Deviation above TL. 81% of the 345 received signals had an upper bound for standard deviation of 6dB. b) Standard Deviation below TL. 93% of the 345 received signals had a lower bound for standard deviation of 3dB.

B. TUNING THE NSPE MODEL

The NSPE model was run by applying the principle of reciprocity, which states, ~~–~~if the location of a small source and small receiver are interchanged in an unchanging environment, the received signal will remain the same" (Kinsler 2000). The resulting TL for each run was then compared with observed TL compiled across all frequencies. Observed versus modeled TL was statistically analyzed to compare 280 different geoacoustic models to determine the best fit geoacoustic model for the shallow region and the best fit geoacoustic model for the deeper, sloping region. The statistics used were: root mean square error (RMSE) for observed versus modeled pressure, the slope of a first order linear regression fit of observed versus modeled pressure, the percent of modeled TL values within one standard deviation of the observed TL. A t-test was also done to determine if the model is biased to be greater than or less than observed TL, and by how much. Lastly, a new metric of TL difference, presented by J. Fabre (2009), was also applied and is presented in Equation 3.1.

$$TL_{difference} = \frac{\sum \left| TL_o(r) - TL_m(r) \right| w(r)}{\sum w(r)}, \qquad (3.1)$$

where the weighting factor is w = 1 if $TL_o \leq 60$ dB, w = $(110\text{-}TL_o)/50$ if TL_o is between 60 and 110 dB, and w = 0 if TL_o is >110 dB.

1. Sediment Layer Variability for Tanner Bank

In the sediment layer, the independent variables were sediment thickness and grain size. The increments for the sediment thickness were 0–6 meters, (based on Bachman, Bucca, and Holzman's research) at 1-meter increments. For the sediment thickness of zero, a very thin layer is actually applied. The grain size was varied from 1.152–3.462 φ, at 0.462-φ increments. These thickness and grain sizes were used to calculate density, compressional sound speed and attenuation, and shear speed and attenuation based on Bachman's equations. Separate runs were made for the geoacoustic

models presented by Bucca and Fulford (1995), Table 2, and were compared with the Bachman based results. A summary of the statistical results for the shallow leg are in Table 3.

Sediment Type	Compressional Speed (m/s)	Compressional Attenuation (dB/m/kHz)	Shear Speed (m/s)	Shear Attenuation (dB/m/kHz)	Density (g/cm^3)
Fine Sand	1700	0.35	420	8.0	1.7
Mud	1470+1.14z	0.06	50	8.0	1.5

Table 2. Values used for the geoacoustic model presented by Bucca and Fulford (1995). The variable z is the depth below the sea floor in meters.

The RMSE values for pressure across most of the geoacoustic models yielded results between 0.605–0.645 μPa. The condition yielding the worst RMSE value for pressure was Bucca's geoacoustic model for a mud bottom. The best condition yielding the lowest RMSE result is Bucca's fine sand model. In terms of grain size, RMSE decreased as φ decreases. There were little to no changes across the thickness variables in the RMSE statistic, with the exception of having no sediment (very thin layer), results are slightly worse.

The slope of the first order linear regression best fit also improved with coarser grain sizes. Across grain sizes, thickness did not affect the slope of the regression line; however, using a thickness of zero yielded regression slopes consistent with other values. Bucca's mud model performed the worst and his sand model had regression slopes near those of the mid-range tested grain sizes.

The most telling statistic was the number of values within one standard deviation observed TL. Bucca's mud model performed worst with only around 25% of modeled TL being within one standard deviation of observed TL. Bucca's sand model performed acceptable with 43% of modeled values within one standard deviation of the observed TL. The statistic improved with the coarser the grain size, to 54% of modeled values within one standard deviation with the coarsest grain size of 1.152 φ. A thickness of 4

meters had the best results, but was only an improvement over other thickness by 1.0 %, however, with no sediment thickness (very thin layer), results went down 6.0%.

To determine bias, a left handed t-test was used. Positive results showing that at a 95% confidence level the average observed p_{rms} was greater than the average modeled p_{rms}. Further investigation to find the model with the least negative bias was done. By incrementally increasing the mean, which the t-test was performed on, the coarsest grain size of 1.152 φ was found to have the smallest mean pressure difference, observed minus modeled, of 0.03 μPa, on a 95% confidence interval.

Using the $TL_{difference}$ metric (Fabre 2009) a similar story was told. For the thickness variable, using a sediment thickness of zero meters produced results on the order of 0.7 dB higher than using a thickness of 1 meter. The sediment thickness of 4 meters produced the best results across all grain sizes. The coarsest grain size produced the best results, and at sediment thickness of 4 meters was 6.16 dB, being within one standard deviation of our upper bound.

Following a review of all of the analyzed statistics it is apparent that using a geoacoustic model following the methods of Bachman, but using the grain sizes provided by Holzman produce modeled TL results closest to those actually observed on range. The statistics for $TL_{difference}$ and percent of values within one standard deviation have better results when the sediment thickness is 4 meters. Table 3 presents a summary of the statistics calculated for the various geoacoustic models, all using a thickness of 4 meters. From Table 3 and Figures 16–18 it can be seen that there is a trend towards better modeled results when using a coarser grain size. Figure 15 is a sample plot of the full field transmission loss, illustrating the interactions with the bottom in this shallow region. This demonstrates the importance for using a geoacoustic model that will result in values closest to observed TL values.

1.152 φ	54.1	6.160	0.6056	0.6866	0.03
1.617 φ	51.9	6.217	0.6064	0.6834	0.035
2.076 φ	50.4	6.304	0.6079	0.6766	0.04
2.538 φ	48.9	6.462	0.6084	0.6725	0.045
3.000 φ	47.4	6.740	0.6101	0.6670	0.05
3.462 φ	42.2	7.382	0.6167	0.6604	0.06
Bucca Sand	43.0	7.399	0.6030	0.6723	0.058
Bucca Mud	24.4	10.838	0.6312	0.6625	0.10
	% of modeled values within one standard deviation	$TL_{difference}$ (dB) (Fabre 2009)	$RMSE_{pressure}$ (μPa)	Slope of 1st order linear regression	Mean difference between observed and modeled pressure with 95% confidence (μPa)

Table 3. Statistical results for the shallow leg geoacoustic models. All results shown are for a thickness of 4 meters, which provided the best results when comparing thickness. The trend of better results by using smaller φ values is apparent.

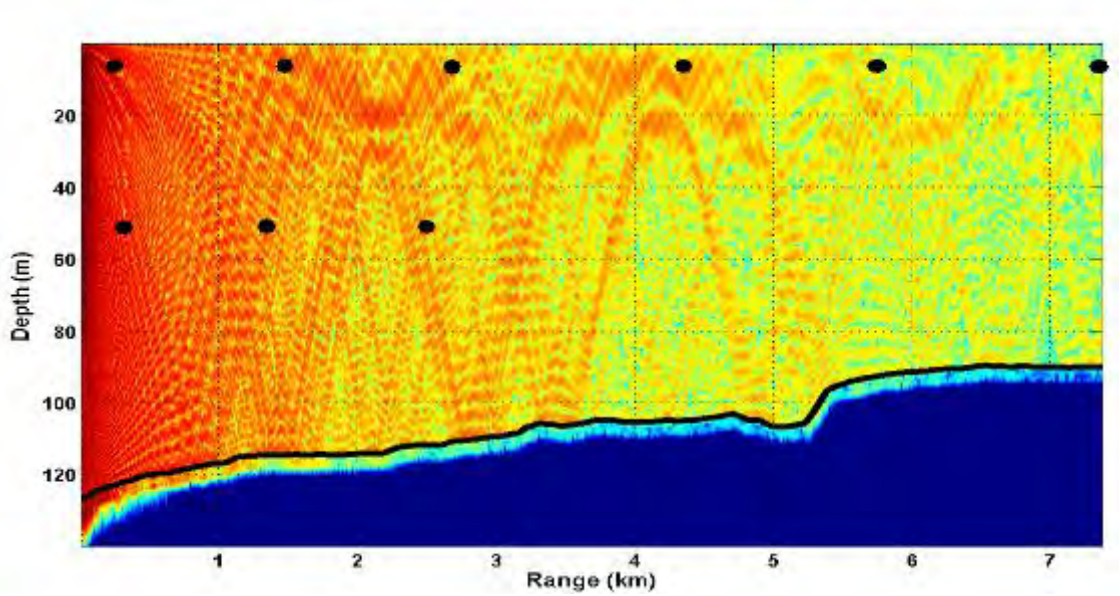

Figure 15. Full field TL plot of the shallow region of Tanner Bank. The heavy black line is the sea floor. The illustration shows the extent of sound penetration into the sediment layer. Source locations are black circles at 6 meter and 50 meter depths. The Acousonde receiver mooring is at the range of 0 km on the left side of the figure.

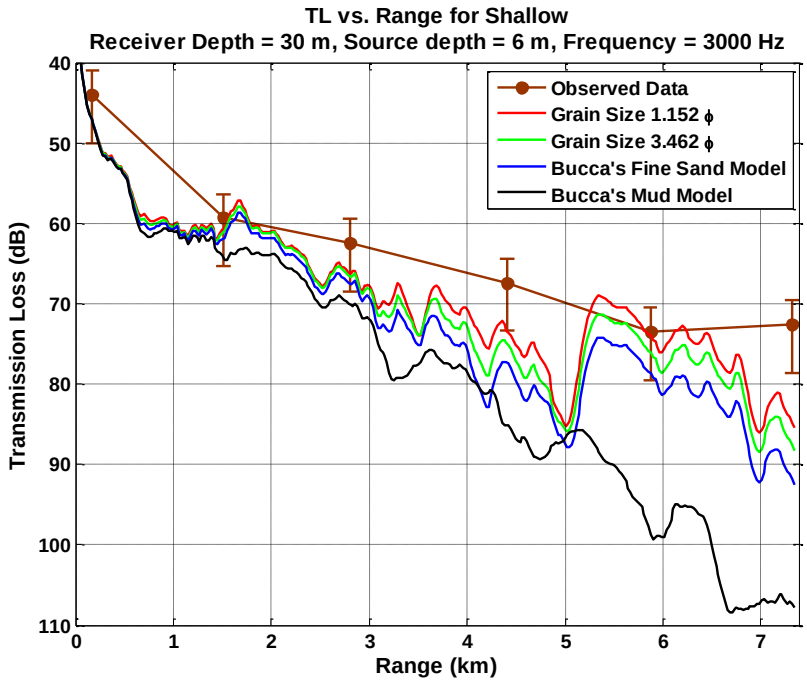

Figure 16. While all of the models have the same trends, minus the mud model with a few deviations, the geoacoustic model with the coarsest grain size yields results closest to observed TL.

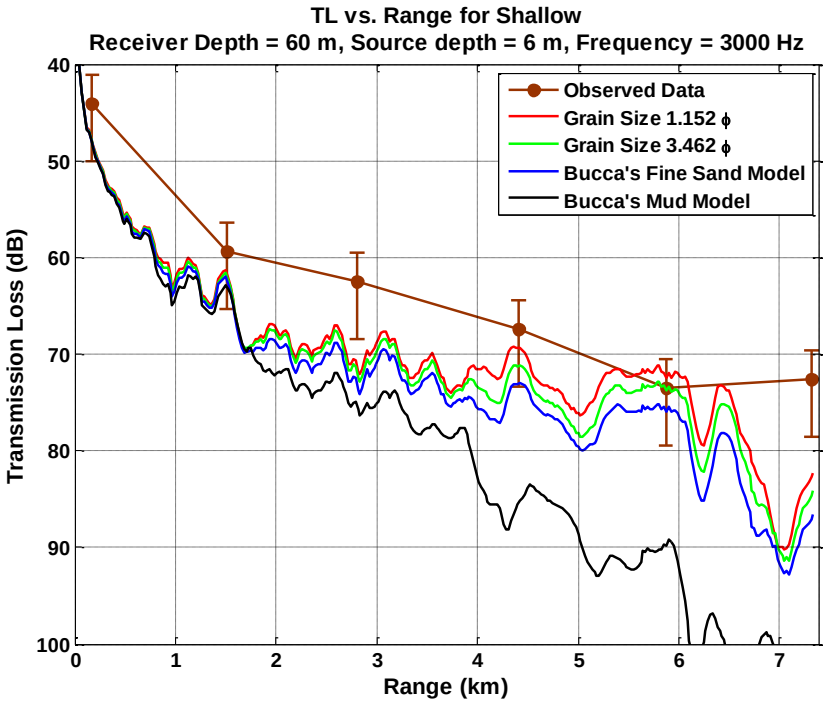

Figure 17. With similar results to the receiver at the 30 meter depth, the receiver at the 60 m depth shows that the best results of modeled TL come from the geoacoustic model using Bachman's equations with the coarsest grain size.

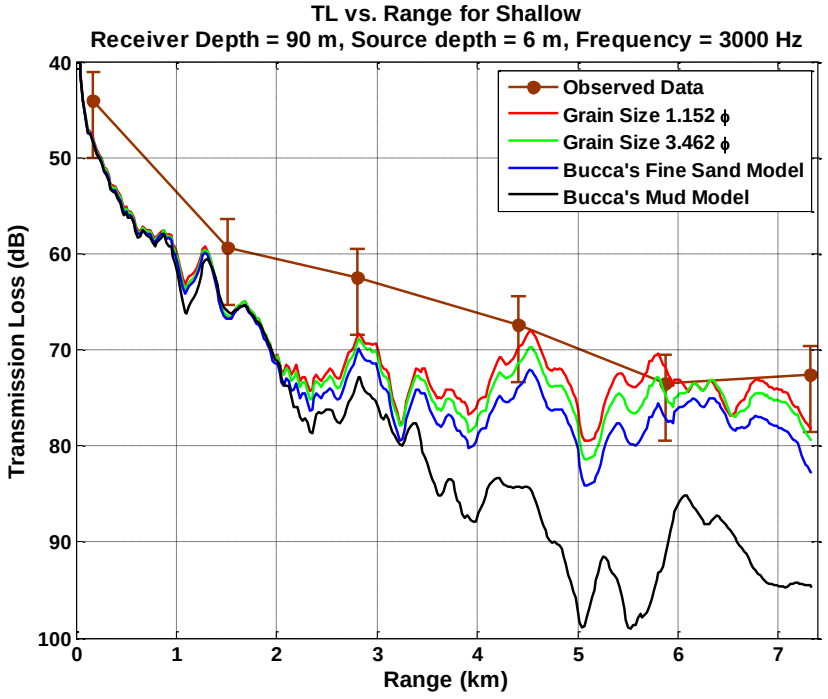

Figure 18. On the bottom receiver, at a depth of 90 meters, the coarsest grain size of 1.152 φ almost comes within one standard deviation a every sampled range.

2. Sediment Layer Variability for the Slope of Tanner Bank

In the sediment layer on the slope, the independent variables were also sediment depth and grain size. The increments for the sediment depths were 75–225 meters at 25-meter increments. The grain size was varied from 2.104–5.724 φ at 0.724 φ increments. These thickness and grain sizes were used to calculate density, compressional sound speed and attenuation, and shear speed and attenuation based on Bachman's equations. Separate runs were made for the geoacoustic models presented by Bucca and Fulford (1995) in Table 2, and were compared with the Bachman based results. A summary of the statistical results for the sloping leg are in Table 4.

The range for RMSE on the slope across the geoacoustic models yielded results between 0.261–0.279 μPa. The RMSE values for pressure showed two trends. RMSE decreased with coarser grain sizes and also decreased with decreasing sediment thickness. The condition yielding the worst RMSE value for pressure was Bucca's geoacoustic model for a mud bottom, which showed no changes with changing sediment thickness. Sediment thickness of 75 meters produced the lowest results for RMSE for all grain sizes and for Bucca's models. RMSE improved with coarser grain sizes; the grain size of 2.104 φ having the lowest RMSE.

The slope of the first order linear regression best fit also improved with coarser grain sizes. The best result was with the coarsest grain size at a sediment thickness of 75 meters. The 75 meter thickness produced first order linear regression slope closest to 1; as thickness changed from 100 meters to 225 meters there was little or no change for the first order linear regression slope. Bucca's mud model performed as well as coarse grains, and Bucca's fine sand model performed as well as the models using mid-sized grains.

The sediment thickness of 75 meters performed the best for the percent of modeled values within one standard deviation of observed TL. The trend for the best grain size leans toward the center as 4.276 φ, with a thickness of 75 meters, has 44.8 % of modeled values within one standard deviation of observed values. Bucca's mud model performed worst with around 25% of modeled TL being within one standard deviation of

observed TL. On the sloping section, Bucca's sand model performed well overall, with 43.8% of modeled values within one standard deviation.

To determine bias, a left-handed t-test was used. Positive results showing that at a 95% confidence level the average observed p_{rms} was greater than the average modeled p_{rms}. Further investigation to find the model with the least negative bias was done. By incrementally increasing the mean, which the t-test was performed on, the coarsest grain size of 2.104 φ was found to have the smallest mean pressure difference, observed minus modeled, of 0.018 μPa, on a 95% confidence interval at the 100 meter thickness.

Using the $TL_{difference}$ showed results of coarse grain sizes yielding the smallest differences. The best results from this metric came from the grain size of 2.828 φ, with a $TL_{difference}$ of 6.5338 dB. Slightly better results came from a thickness of 75 meters across all grain sizes. Bucca's mud model performed horribly, where his fine sand model performed as well as the mid-grain models tested.

Following a review of all of the analyzed statistics for the sloping leg it is apparent that using a geoacoustic model following the methods of Bachman, but using the grain sizes provided by Holzman produce modeled TL results closest to those actually observed on range. All of the statistics, with the exception of the t-test performed best at a thickness of 75 meters. The t-test performed best at 125 meters. The results presented in Table 4 are for a sediment thickness of 75 meters. From Table 4 and Figures 20–22 it can be seen that there is a trend towards better modeled results when using a coarser grain size. Figure 19 is a sample plot of the full field transmission loss, illustrating the interactions with the bottom in this sloping region. Due to fewer bottom interactions a complicated formula for geoacoustics is not as critical, which is why Bucca's model for the fine sand bottom performs acceptably well for a model with reduced complexity.

2.104 φ	43.3	6.6603	0.2613	0.7582	0.018
2.828 φ	43.8	6.5338	0.2627	0.7507	0.03
3.552 φ	43.8	6.6099	0.2701	0.7424	0.035
4.276 φ	44.8	6.6462	0.2729	0.7387	0.0365
5.000 φ	42.4	6.6977	0.2674	0.7443	0.035
5.724 φ	43.3	6.8154	0.2684	0.7444	0.0363
Bucca Sand	42.4	7.0248	0.2699	0.7435	0.0367
Bucca Mud	21.0	14.8128	0.2784	0.7518	0.085
	% of modeled values within one standard deviation	$TL_{difference}$ (dB) (Fabre 2009)	$RMSE_{pressure}$ (µPa)	Slope of 1st order linear regression	Mean difference between observed and modeled pressure with 95% confidence (µPa)

Table 4. Statistical results for the sloping leg. All results shown are for a sediment thickness of 75 meters, which provided the best results when comparing statistics across thickness values holding grain size constant. The more coarse grain sizes provide the best statistics, although there is not one-grain size that dominates across all statistics.

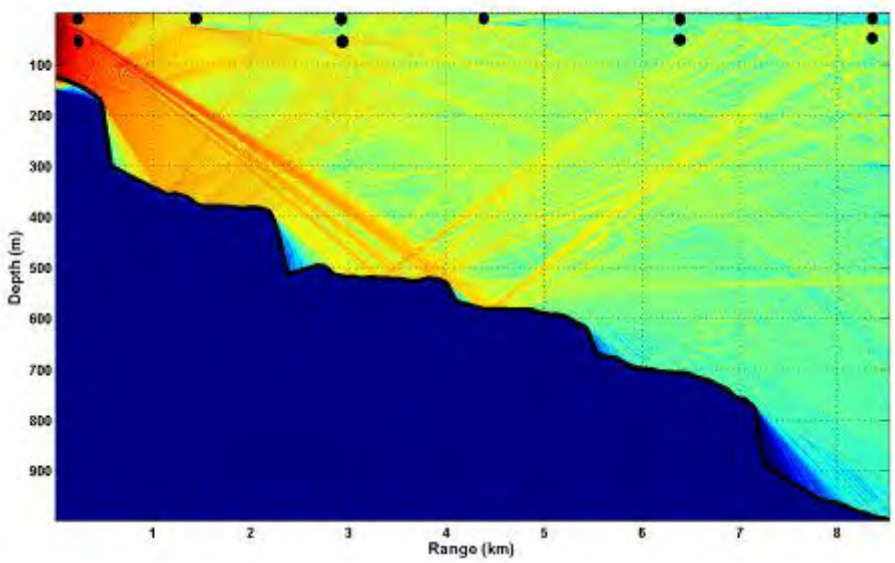

Figure 19. Full field TL plot of the sloping region of Tanner Bank. The heavy black line is the sea floor. The illustration shows that with fewer bottom interactions than on Tanner Bank itself, there is a lesser extent of sound penetration into the sediment layer. Source locations are black circles at 6 meter and 50 meter depths. The Acousonde receiver mooring is at the range of 0 km on the left side of the figure.

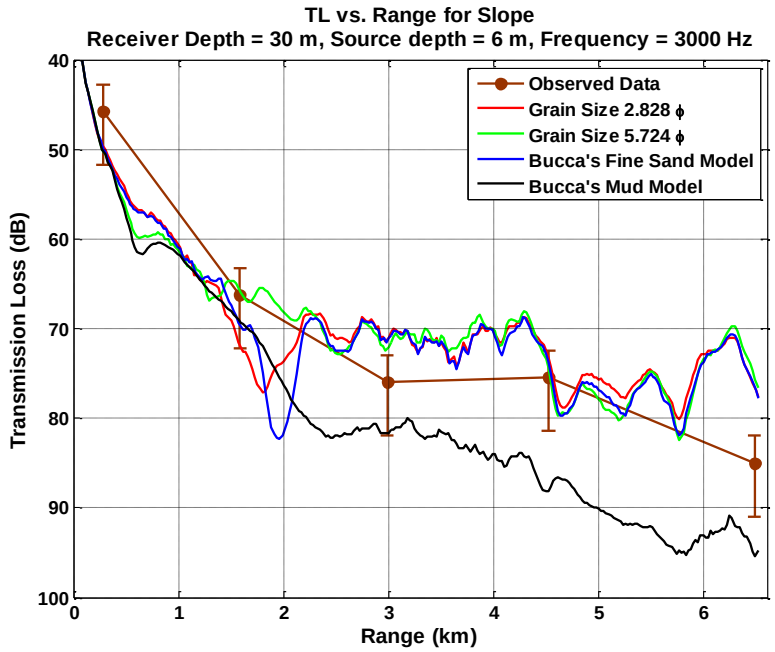

Figure 20. The top receiver, 30 meters deep, along the slope, shows little difference between geoacoustic models, with the exception of the mud bottom, which gets worse with increased range.

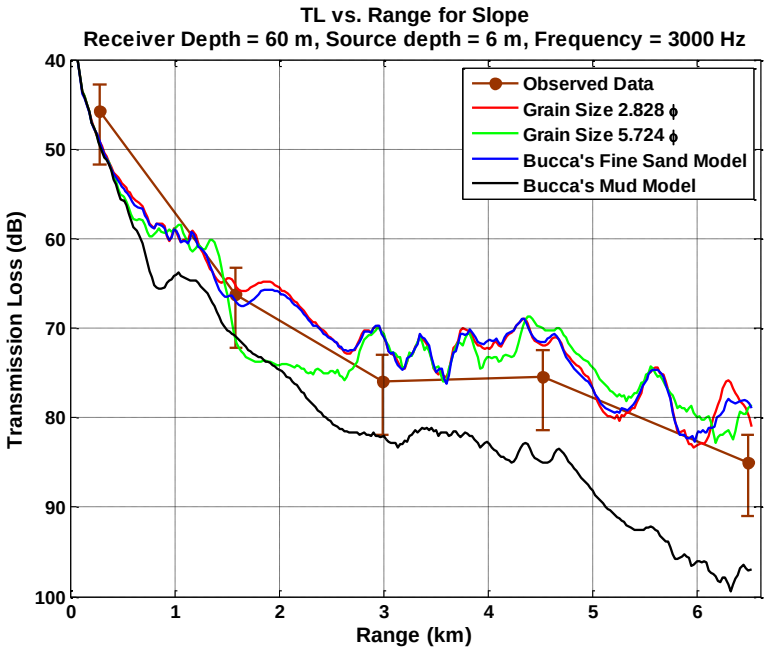

Figure 21. The coarse grain size of 2.828 φ, and Bucca's fine sand model are consistent with each other and statistically produce results of modeled TL closest to observed TL.

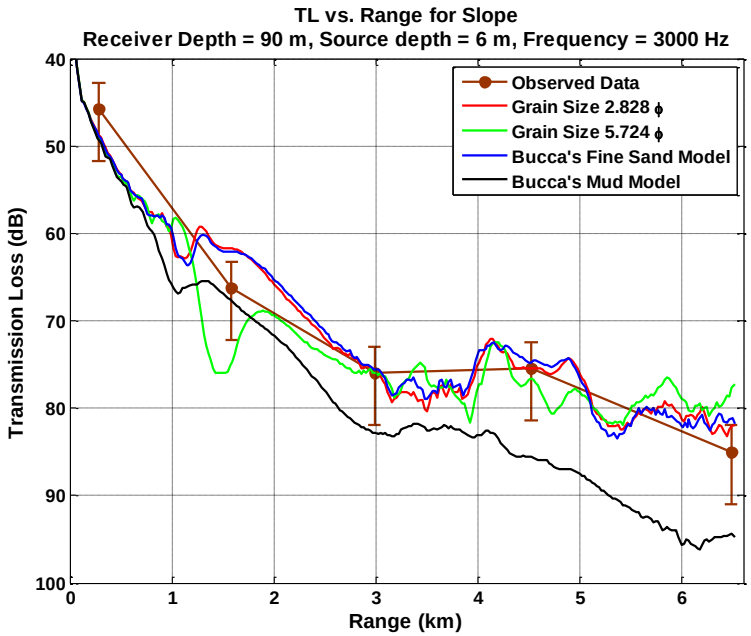

Figure 22. This illustration of the modeled TL to the bottom receiver at 90 meters deep, along the slope, shows why the fine grain size, 5.724 φ, model does not statistically perform well. For the 5.724 φ curve, a large fluctuation occurs at 1.5 km, with smaller yet noticeable deviations at 4.5, and 5.5 km.

3. Rock Layer Variability

The compressional sound speed in the underlying rock was varied from 2300–2500 m/s with a constant compressional attenuation factor of 0.009 dB/m/kHz. Between Bucca's and Bachman's models, there is little difference in shear sound speed, therefore it was held constant at 885 m/s for models with varied grain sizes. The shear attenuation factor was held at 3.4 dB/m/kHz, for all models with grain sizes. A constant density of 2.21 g/cm^3 was used for all models. Across all statistics analyzed there were no trends or significant differences for any values of compressional sound speed. A conclusion can be drawn that with any compressional sound speed used from 2300–2500 m/s the NSPE model will not yield significantly different values for TL in the region of Tanner Bank. The inputs for the deeper sloping section of Tanner Bank were the same with regards to the compressional sound speed, attenuation, and density of the underlying rock layer.

THIS PAGE INTENTIONALLY LEFT BLANK

IV. CONCLUSIONS

The objective of this thesis was to find a geoacoustic model to use in SCORE near Tanner Bank. The results are conclusive that a geoacoustic bottom developed using Bachman's equations with coarse grain sizes yield modeled TL values closest to observed TL values. The best geoacoustic model has greater than 50 percent of its modeled values within one standard deviation of observed values, based solely on the time dependence of source level. When viewing the TL versus range plots, (Figures 16–18 and 20–22) it can be seen that there are several instances where modeled TL would be even closer to observed TL if a range factor were considered in the standard deviation. There are other factors contributing to differences between modeled and observed values, which were not tested in this thesis, such as a range or time dependent wind speed, better bathymetry, or range dependent geoacoustics.

For the shallow leg, directly over Tanner Bank, it is concluded that a geoacoustic model of the sediment layer be constructed using Bachman's equations and a sediment grain size on the order of 1.15 φ (0.45 mm). Even more coarse grain sizes should be chosen with decreasing ocean depth as proposed by Holzman. While the sediment thickness may be nonexistent in areas, and of varying thickness in others, using a thickness of 4 meters for a geoacoustic model in the shallow regions (near 100 meters deep) of SCORE produce the modeled TL values closest to those observed. Even though Bucca and Bachmann present different geoacoustic models for the underlying rock layer in SCORE, these two models for the rock layer produced results, which were statistically insignificant.

For the sloping leg, from 100–1000 meters deep, it is concluded that a geoacoustic model be constructed using a sediment thickness of 75 meters. Applying Bachman's equations, a grain size on the order of 2.10 φ (0.23 mm) should be used in order to give modeled transmission loss values closest to those observed. If a less complex geoacoustic model is desired, the fine sand model presented by Bucca should be used, expecting only slightly less accurate results. These recommendations are made

based on the fact that three of the five statistics analyzed had better results with the coarsest grain size and the other two statistics were still producing more favorable results using coarser grain sizes.

IV. FUTURE RESEARCH

A. ANALYSIS OF OTHER DATA SETS

During the cruise aboard R/V Sproul, a HARP was deployed at the northern end of the sloping leg acoustic profile. This data can be used to confirm and refine the conclusions presented in this thesis as to the structure of the geoacoustics for the area. Data from the HARP will be available after recovery, expected in November 2011. Data from the transmissions presented in this thesis were also collected on several hydrophones at the western edge of SOAR, operated by the U.S. Navy. This data is currently being converted to usable formats for analysis.

B. ANALYSIS OF OTHER AREAS

This experiment also should to be replicated in other areas of SCORE. Deeper tracks should be covered where the bathymetry is consistently 1000 meters or greater. Observed transmission loss studies of SCORE should be done with changing bathymetry (deep to shallow, then back to deep). Models of a changing bathymetry then should be created with range dependent geoacoustics. Results from these future experiments should then be compared to the results in this thesis to decide if geoacoustics in and near SCORE can should be generalized to achieve good results, or, should geoacoustics in and near SCORE be made as specific and range dependent as possible to achieve the best results possible. Similar research should also be conducted in other Navy ranges such as the proposed Under Sea Warfare Training Range (USTWR), off the coast of Jacksonville, Florida.

THIS PAGE INTENTIONALLY LEFT BLANK

LIST OF REFERENCES

Bachman, R. T., 1994: A Three-Dimensional Geoacoustic Model for the Catalina Basin. NRaD Technical Report 1669, 60.

Bucca, P. J., and J. K. Fulford, 1995: Environmental Variability During the Tanner Bank Phase of the Pacific Coast Operation. NRL/MR/7182--95-7578, 18.

Collins, M. D., 1993: A split-step Padé solution for the parabolic equation method. *J. Acoust. Soc. Am.*, **93**, 1736–1742.

Fabre, J. Paquin, 2009: A metric for comparing acoustic transmission loss curves. *OCEANS 2009, MTS/IEEE Biloxi - Marine Technology for Our Future: Global and Local Challenges,* [Available online at http://ieeexplore.ieee.org/stamp/stamp.jsp?tp=&arnumber=5422312&isnumber=5422059]

Greeneridge Sciences, Inc. 2011: FAQs Technical. [Available online at http://www.acousonde.com/faqtechnical.html]

Hamilton, E. L., 1980: Geoacoustic modeling of the sea floor. *J. Acoust. Soc. Am.*, **68**, 1313–1340.

Holzman, J. E., 1952: Submarine Geology of Cortes and Tanner Banks. *J. Sediment. Petrol*., **22**, 97–118.

Kinsler, L. E., Frey, A. R., Coppens, A. B., and Sanders, J. V., 2000: *Fundamentals of Acoustic.* 4th ed. John Wiley and Sons, 548 pp.

Lockheed Martin Maritime Systems and Sensors, 2005: Expendable Bathythermograph Brochure, 4.

Larsen, M. A., and Hovem, J. M., 2007: Geoacoustic inversion. *Buried Waste in the Seabed—Acoustic Imaging and Bio-toxicity*, Blondel, P., and Caiti, A. Springer, 105–111.

Mackenzie, K. V., 1981: Nine-term equation for sound speed in the oceans. *J. Acoust. Soc. Am.*, **7**, 807–812.

Naval Oceanographic Office Systems Integration Department, 2009: Split-Step Fourier/RAM Parabolic Equation Model Version 5.5(U). Naval Oceanographic Office.

Naval Undersea Warfare Center, 2011: G-34 Technical Publication. [Available online at http://www.navsea.navy.mil/nuwc/newport/usrdiv/Transducers/G34.pdf]

Saunders, P. M., 1981: Practical Conversion of Pressure to Depth. *J. Phys. Oceanogr.*, **11**, 573–574.

Urick, R. J., G. R. Lund, and D. L. Bradley, 1969: Observations of fluctuation of transmitted sound in shallow water. *J. Acoust. Soc. Am.*, **45**, 683–690.

INITIAL DISTRIBUTION LIST

1. Defense Technical Information Center
   Ft. Belvoir, Virginia

2. Dudley Knox Library
   Naval Postgraduate School
   Monterey, California

3. Dr. Jeff Paduan
   Naval Postgraduate School
   Monterey, California

4. Dr. Ching-Sang Chiu
   Naval Postgraduate School
   Monterey, California

5. CDR John Joseph (Retired)
   Naval Postgraduate School
   Monterey, California